Biomaterials Advances 159 (2024) 213815

Contents lists available at ScienceDirect

Biomaterials Advances

journal homepage: www.journals.elsevier.com/materials-science-and-engineering-c

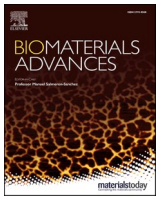

Ionized jet deposition of silver nanostructured coatings: Assessment of chemico-physical and biological behavior for application in orthopedics

Gabriela Graziani [a,*,1], Daniele Ghezzi [a,b,1], Marco Boi [a], Nicola Baldini [a,c], Enrico Sassoni [d], Martina Cappelletti [b], Giorgio Fedrizzi [e], Melania Maglio [f], Francesca Salamanna [f], Matilde Tschon [f], Lucia Martini [f], Stefano Zaffagnini [g], Milena Fini [h], Maria Sartori [f]

[a] BST-NaBi Biomedical Science and Technologies Laboratory and Nanobiotechnology, IRCCS Istituto Ortopedico Rizzoli, Via di Barbiano 1/10, 40136 Bologna, Italy
[b] Department of Pharmacy and Biotechnology, University of Bologna, Via Irnerio 42, 40126 Bologna, Italy
[c] Department of Biomedical and Neuromotor Sciences, University of Bologna, Via Massarenti 9, 40128 Bologna, Italy
[d] Department of Civil, Chemical, Environmental and Materials Engineering, University of Bologna, Via Terracini 28, 40131 Bologna, Italy
[e] Istituto Zooprofilattico Sperimentale della Lombardia e dell'Emilia-Romagna (IZSLER), Reparto Chimico degli Alimenti, Via Pietro Fiorini 5, 40127 Bologna, Italy
[f] Surgical Sciences and Technologies, IRCCS Istituto Ortopedico Rizzoli, Via di Barbiano 1/10, 40136 Bologna, Italy
[g] II Orthopaedic and Traumatologic Clinic, IRCCS Istituto Ortopedico Rizzoli, via Pupilli 1, 40136 Bologna, Italy
[h] Scientific Direction, IRCCS Istituto Ortopedico Rizzoli, Via di Barbiano 1/10, 40136 Bologna, Italy

ARTICLE INFO

Keywords:
Anti-infective coating
Infection
Bone prosthesis
Thin film
Plasma assisted techniques
Nanostructured coating

ABSTRACT

Infection is one of the main issues connected to implantation of biomedical devices and represents a very difficult issue to tackle, for clinicians and for patients. This study aimed at tackling infection through antibacterial nanostructured silver coatings manufactured by Ionized Jet Deposition (IJD) for application as new and advanced coating systems for medical devices. Films composition and morphology depending on deposition parameters were investigated and their performances evaluated by correlating these properties with the antibacterial and antibiofilm efficacy of the coatings, against *Escherichia coli* and *Staphylococcus aureus* strains and with their cytotoxicity towards human cell line fibroblasts. The biocompatibility of the coatings, the nanotoxicity, and the safety of the proposed approach were evaluated, for the first time, *in vitro* and *in vivo* by rat subcutaneous implant models. Different deposition times, corresponding to different thicknesses, were selected and compared. All silver coatings exhibited a highly homogeneous surface composed of nanosized spherical aggregates. All coatings having a thickness of 50 nm and above showed high antibacterial efficacy, while none of the tested options caused cytotoxicity when tested *in vitro*. Indeed, silver films impacted on bacterial strains viability and capability to adhere to the substrate, in a thickness-dependent manner. The nanostructure obtained by IJD permitted to mitigate the toxicity of silver, conferring strong antibacterial and anti-adhesive features, without affecting the coatings biocompatibility. At the explant, the coatings were still present although they showed signs of progressive dissolution, compatible with the release of silver, but no cracking, delamination or *in vivo* toxicity was observed.

1. Introduction

Infection and the correlated inflammatory microenvironment are among the most frequent and severe complications in the healthcare system [1,2]. The risk of infection demands a high level of attention especially when implantation of biomedical devices is involved, such as orthopedic prostheses and percutaneous implants. This latter approach is common for the treatment of several bone related conditions and its use is constantly growing. Among the expanding and most challenging fields, stand the systems for direct skeletal attachment for prosthetic

* Corresponding author.
E-mail addresses: gabriela.graziani@polimi.it (G. Graziani), daniele.ghezzi@unibo.it (D. Ghezzi), marco.boi@ior.it, nicola.baldini@ior.it (M. Boi), enrico.sassoni2@unibo.it (E. Sassoni), martina.cappelletti2@unibo.it (M. Cappelletti), giorgio.fedrizzi@izsler.it (G. Fedrizzi), melania.maglio@ior.it (M. Maglio), francesca.salamanna@ior.it (F. Salamanna), matilde.tschon@ior.it (M. Tschon), lucia.martini@ior.it (L. Martini), stefano.zaffagnini@ior.it (S. Zaffagnini), milena.fini@ior.it (M. Fini), maria.sartori@ior.it (M. Sartori).
[1] Gabriela Graziani and Daniele Ghezzi contributed equally to this work and share first authorship.

https://doi.org/10.1016/j.bioadv.2024.213815
Received 19 July 2023; Received in revised form 21 February 2024; Accepted 23 February 2024
Available online 25 February 2024

limb in amputee patients. Indeed, in this latter application, it is necessary to permanently cross the epithelial barrier for connecting the external limb to the residual bone element [3], but breaching the skin expose patients to an increased risk of infection development, both superficial and deep. The treatment of infection in any anatomical district represents a very difficult task, both for clinicians and patients, leading to high economical and societal burden [4,5]. In the case of osteointegrated prostheses for amputees, this is further challenging, since any revision surgery requires to increase the depth of amputation. To tackle infection, a systemic prophylaxis is performed. However, the phenomenon of antibiotic resistance progressively conditioning one of the major weapons of defense and treatment against bacterial infections, *i.e.*, the antibiotics [6].

Hence, although controlled antibiotic release systems, such as antibiotic impregnated devices or antibiotic loaded coatings can be a promising alternative to systemic therapy, as they allow to deliver higher concentrations of antibiotics directly in the infection site, they do not address bacterial resistance, and the ever increasing rise this phenomenon is making them increasingly ineffective [7,8]. In addition, both systemic antibiotic therapy (gold standard) and local application of organic antibiotics have some drawbacks that limit their efficacy, mainly linked to systemic toxicity, insufficient control over elution duration and extent.

The treatment of infections becomes particularly challenging when biofilm forms, that protects the microorganisms from the host immune system and from antimicrobial compounds, while allowing bacterial proliferation and spreading [9,10]. Hence, the actuation of prevention strategies and the development of new therapeutic approaches to tackle antimicrobial resistance are the focus of intensive research.

In this scenario, the use of inorganic antimicrobial coatings able to locally deliver antibacterial agents directly in the site of insertion without causing bacterial resistance appears extremely appealing [10]. To this aim, among several options proposed in the literature, the modification of implants surface by inorganic thin, nanostructured coatings with tunable composition and physicochemical properties, appears particularly promising to overcome microbial resistance [11] and prevent the occurrence of infection [12]. Ideal antibacterial coatings should be multi-spectral and able to locally deliver antibacterial agents directly in the site of insertion, for a suitable time and in an appropriate concentration, without causing cytotoxicity or bacterial resistance [12]. Among the inorganic compounds having antibacterial efficacy, silver (Ag) is by far the most investigated, as it is active against several bacterial strains (over 650), including drug-resistant ones [13]. Therefore, antibacterial Ag-coatings are largely studied in the literature and used in the clinical practice, for catheters, gauzes, sutures, prostheses, and a variety of implantable and non-implantable biomedical devices [14–40].

Because Ag-coatings are so extensively used, a variety of procedures have been proposed for their deposition, also depending on substrate morphology and composition. While the firstly developed methods relied on simple immersion in liquid precursors, more recently, several techniques have been developed, such as pulsed laser deposition and magnetron sputtering, concentrating on manufacturing nanostructured thin films with a fine control over films characteristics [14]. In fact, despite their diffusion, traditional Ag-coatings exhibit some drawbacks that have limited their efficacy, either connected to scarce adhesion or control over film uniformity and thickness, all possibly leading to cracking and detachments, and/or to insufficient control over ion release, which, in turn, determines efficacy and cytotoxicity [41]. To overcome these issues, thickness at the nanoscale and nano-structuring are pursued, to reduce films tendency to cracking and delamination, and achieve a fine control over Ag release, respectively.

The Authors have recently proposed the use of pulsed electron deposition (PED) and its novel modification, ionized jet deposition (IJD) for manufacturing nanostructured thin films for biomedical devices [42–47]. IJD shows important advantages for antimicrobial functionalization of implants, since it permits to obtain submicrometric thin films (avoiding mechanical mismatch with the implant leading to cracking and detachments), having a nanostructured surface morphology (permitting tuning of ion-release) and a high fidelity in the conservation of stoichiometry from the deposition target to the coating, also for complex materials [48]. In addition, excellent adhesion was found for all substrate and target combinations (bioglass, zirconia, hydroxyapatite on both metal and polymers). Preliminary studies on Ag films, manufactured by IJD by direct ablation of metallic Ag targets, have thoroughly characterized the morphology of the coatings, depending on the deposition conditions. In those studies, coatings morphology and growth dynamics of the films had been characterized by Atomic Force Microscopy (AFM) and Scanning tunnelling microscopy (STM) [38], highlighting that coatings exhibit a very uniform nanostructured morphology, as they are composed of spherical aggregates of 10–20 nm in diameter and a submicrometric thickness. In addition, we demonstrated that the coatings can be used to functionalize electrospun patches and provide them with antibacterial efficacy [49].

Thanks to nanostructuring, superior properties are expected compared to traditional coatings, for what regards the cytotoxicity and the extent and duration of antibacterial activity. In addition, by using metallic Ag coatings, which release Ag ions, instead of nanoparticles, we expect to overcome possible cytotoxicity and nanotoxicity of the films. For this reason, in the present study, for the first time we propose the used of these new nanostructured antibacterial thin films for orthopedic and percutaneous applications and we assess their biological behavior. The characteristics of the coatings are correlated to their cytotoxicity and antibacterial and antibiofilm efficacy against both gram-positive and gram-negative strains. Based on these results, the most promising coatings are selected and their *in vivo* histocompatibility is further investigated by subcutaneous implant in rat model. Finally, although nanotoxicity is not expected, it cannot be indeed excluded *a priori*, as possible the detachment of nanoscale fragments could lead to their accumulation in target organs. For this reason, nanotoxicity *in vivo* - a crucial aspect still remaining largely unexplored in literature and representing a further key element of novelty - especially regarding nanostructured coatings, was specifically investigated, by assessing their possible accumulation in target organs by ICP-MS.

2. Materials and methods

2.1. Substrate materials

Coatings were deposited onto 5 mm diameter cylinders of Ti_6Al_4V alloy (grade 23 ELI), to mimic standard composition and surface roughness of orthopedic implants (Ra 5 μm) (Zare s.r.l, Boretto (RE), Italy and Citieffe S.r.l., Bologna, Italy), for *in vitro* investigations. For *in vivo* study, Ti_6Al_4V discs of 10 mm in diameter and 1 mm in thickness were adopted, having the same composition, surface roughness and finishing of the cylinders (Cizeta Surgical, San Lazzaro, Bologna, Italy).

2.2. Coating deposition

Ag thin films were deposited by IJD (Noivion Srl, Rovereto (TN), Italy). Cylindrical silver targets (Ø = 30 mm, thickness = 7 mm, purity rate 99.999 % - Kurt J. Lesker, PA, USA) were used for the deposition, mounted on a rotating holder. Deposition parameters were selected based on preliminary tests, aimed at optimizing coatings uniformity and achieving a suitable deposition rate. Deposition was carried out at room temperature.

Different deposition times have been selected: 10, 20, 30, 45 and 60 min, corresponding to different film thicknesses. Deposition times below 10 min and above 60 min were discarded, as preliminary SEM investigation evidenced insufficient uniformity and/or tendency to crack.

Samples were labelled based on deposition time as Ag10, Ag20, Ag30, Ag45, and Ag60.

2.3. Coating characterization

Coatings morphology has been characterized by Field Emission Gun Scanning Electron Microscopy (FEG-SEM, Tescan Mira3, CZ, working distance = 10 mm, voltage = 10 kV). Based on FEG-SEM images at 50.000× magnification, the dimension of the aggregates that constitute the coatings was measured by ImageJ software (National Institutes of Health, USA). Coatings composition was evaluated by Energy Dispersive X-ray Spectroscopy (EDS), using a Bruker probe coupled with the FEG-SEM. EDS composition was tested in 3 different areas of 2 samples, to assess presence of silver coatings. To measure the uniformity and substrate coverage of the films, maps were also acquired.

2.4. In vitro cytotoxicity

The cytotoxicity of the antibacterial nanostructured coatings was evaluated according to the international standard UNI EN ISO 10993 - Part 5 (2009) "Tests for in vitro cytotoxicity" to determine *in vitro* biological response and the presence of any acute damage caused by these new coatings on cells. Human immortalized fibroblasts BJ5ta cells (ATCC® CRL-4001™) were expanded at 37 °C in a humidified atmosphere with 5 % CO_2 (4:1 mixture of DMEM: Medium 199 with addition of 0.01 mg/mL of hygromycin B and 10 % FCS). Upon reaching 80 % confluence, cells were detached, counted, and suspended at the final concentration of 30,000 cells/well in 24-well plates and left to adhere for 24 h to obtain a uniform cell monolayer. Then, the culture medium was changed and Ag10, Ag20, Ag30, and Ag60 discs were placed in direct contact with cell monolayer, in comparison to uncoated Ti_6Al_4V (hereinafter identified as CTRM). BJ5ta cells not in contact with the tested coatings, were used as a negative control (CTRneg), while BJ5ta cells treated with a toxic agent (1 % phenol dissolved in the medium) as positive control (CTRpos).

Fibroblasts metabolic activity was quantified at 72 h by means of the Alamar Blue assay Invitrogen (Termo Fisher Scientific, Waltham, Massachusetts, US). The fluorescence signal emitted by the cell's cultures with silver nanostructured coating and control conditions was measured by a spectrophotometer (iMARK spectrophotometer, Biorad) at a wavelength of 570/625 nm. The obtained values were converted to a percentage of reduction of the Alamar Blue reagent adopting a specific formula and normalized for the values obtained for the CTRneg. In addition, the release of intracellular enzyme Lactic Dehydrogenase (LDH) as result of damage to the cells membrane was also measured in the culture medium. The amount of LDH released into the culture medium was measured adopting the Cytotoxicity Detection Kit (Roche Diagnostics GmbH Roche Applied Science Mannheim, Germany). According to the manufacturer's protocol, collected cells supernatant from each experimental condition was incubated with the reaction mix for 30 min in the dark and the colorimetric reaction was spectrophotometrically measured (iMARK spectrophotometer, Biorad) at a wavelength of 490 nm. The measured values were then expressed as % of cytotoxicity. Finally, fibroblasts were stained with vital non-toxic Neutral Red (NR) dye solution (Sigma-Aldrich, St. Louis, MI, USA) for the qualitative evaluation of the overall morphology of the culture. This test provides qualitative information about cells morphology, membrane integrity and, indirectly, on viability, by providing an additional parameter for assessing the potential cytotoxicity of the nanostructured Ag-coatings.

2.5. In vitro antibacterial efficacy

2.5.1. Bacterial cultures preparation

Two pathogenic bacteria were tested, *i.e.*, the gram-negative *Escherichia coli* ATCC® 8739™ and the gram-positive *Staphylococcus aureus* ATCC® 6538P™. All cultures were conducted using Luria-Bertani (LB) medium, to which agar (1.5 % *w/v*) was added to generate solid LB plates. The study was carried out by inoculating a single colony of each strain (grown on agar plate for 24 h) in 50-mL tubes with 5 mL of LB liquid medium. Cultures were grown overnight at 37 °C under shacking at 130 rpm and then diluted to reach specific optical density values, measured at 600 nm (OD_{600}).

2.5.2. Antibacterial assay of ag-coated discs

To evaluate the antibacterial activity of Ag-coated discs, the overnight-grown bacterial cultures were diluted to reach a final concentration of ~10^6 CFU/mL. The Ag-coated and non-coated discs were placed at the bottom of 48-wells microplates that were filled with 500 μL of bacterial suspension and incubated for additional 8 h at 37 °C under shaking conditions (130 rpm). Serial dilutions and enumeration on LB agar plates were performed at different time points to assess the bacterial growth by counting the number of Colony Forming Units (CFUs). Each experiment was performed in triplicate.

2.5.3. Antibiofilm assay of ag-coated discs

To measure the antibiofilm activity of Ag-coated discs, the bacterial cultures were diluted to reach OD_{600} = 0.03. Ag-coated and non-coated discs were transferred with 500 μL of each bacterial suspension in 48-wells microplates. Microplates were incubated for 48 h at 37 °C under gentle shaking (50 rpm). The coated/uncoated samples were removed from the cultures and rinsed twice with 0.85 % NaCl (*w/v*) to wash away the non-attached cells. The sessile cells were first fixed with 99 % ethanol (v/v) for 10 min and then stained with 0.2 % crystal violet (w/v), incubated for 10 min at room temperature. The excess of unbound crystal violet was removed by washing the discs three times with sterile water. The bound dye was extracted with 33 % acetic acid (v/v). The amount of the biofilm formation was measured at OD_{595} The background staining was corrected by subtracting the mean value of the absorbance of the target wells with the absorbance detected in the negative controls (wells filled with the growth medium, but without bacterial inoculation). The inhibition of bacterial biofilm (% inhibition in Fig. 5) was calculated as follows: % inhibition = (1 - T/C) x 100, where T and C are the biofilm density (measured as OD_{595}) in the target experimental samples (discs with coatings) and control samples (discs without coatings), respectively. Each experiment was performed in triplicate.

2.6. In vivo histocompatibility and systemic toxicity assessment

2.6.1. In vivo experimental design

The *in vivo* study was performed complying with Italian and local regulations (Italian Law on animal use for scientific purpose). All tests were disciplined by the research protocol authorized from the Ethic Committee of Rizzoli Orthopedic Institute and by the Italian Ministry of Health (n° 44/2016-PR) in agreement with Law by Decree 26/2014. Based on the results obtained from the previous cytotoxicity and microbiological investigations (cfr. §2.4, 2.5), Ag45 and Ag60 have been selected to be studied in an *in vivo* model. Ten male Sprague Dawley rats, b.w. 235 ± 5.1 g, purchased from authorized farm (Charles River Laboratories, Italia, Srl) and submitted to a quarantine period, were used for the subcutaneous implantation of uncoated control, Ag45 and Ag60 discs. Animals were grouped in cages with enriched materials with free access to food and water. The *in vivo* study was performed according to the standard method suggested in UNI EN ISO 10993 - Part 6 (2017) "Tests for local effects after implantation". All implanted materials (discs coated with Ag nanostructured coatings and uncoated controls discs) were gamma-ray sterilized at 25 kGy prior to the *in vivo* implant procedures.

2.6.2. Surgical procedures and ex-vivo investigations

Surgical implants were performed under general anesthesia induced by intramuscular injection of ketamine (87 mg/kg) and xylazine (3 mg/kg). After shaving the dorsal region and setting up the operating field, four small incisions were performed per animal, two on each side, taking the midline of the animal back as a reference. Four subcutaneous pockets

were created by gentle dissection at a minimum distance of 1 cm from each other. The Ag-coated discs (on the right side) and controls (left side) discs were positioned in each pocket. Five rats were implanted with Ag45 and the other 5 with Ag60 to obtain 10 implant sites for each type of coating. At the end of the positioning procedures, the incisions were sutured, and the surgical wounds were medicated. Postoperatively, antibiotic and analgesic therapy was administered, and the animals were checked to evaluate their general clinical conditions.

At 4 weeks, under general anesthesia, each rat underwent a cardiac withdrawal of 5 mL of blood, then was immediately euthanized with i.v. injection of Tanax (Hoechst AG, Franfurt-am-Main, Germany). Then, kidneys, spleen, liver, lungs, heart and brain (brain, midbrain, cerebellum and brain bridge) were retrieved for the assessment of systemic toxicity and the subcutaneous implant sites for the macroscopic, histological and histomorphometric analyses. The blood samples and organs were weighed, identified, and immediately frozen at −20 °C to be processed by ICP-MS analysis at the Reparto Chimico degli Alimenti of IZSLER. For histological investigations, the retrieved samples were fixed in 10 % buffered formalin for 24 h at room temperature with discs in place. After the fixation procedure, all discs were gently removed, and tissues were processed to be embedded in paraffin according to the standard histological procedure. Histological sections of 5 μm thickness were obtained from each site of implant using a HM340 microtome (Microm International GmbH, Germany). Sections were stained with Hematoxylin and Eosin and acquired using the Aperio digital scanning system (AperioScanscope AT2 System, Aperio Technologies, Vista, CA - USA) at maximum resolution. The semi-quantitative score reported in the ISO 10993-6 standard was applied to evaluate cells and tissue response to nanostructured Ag-coatings in comparison to control discs. The evaluations included, but were not limited to, assessing the presence of fibrosis/fibrous capsule, the inflammatory state of the tissue (based on the types of detected inflammatory cells, presence, extent, and type of tissue necrosis, presence of fatty infiltration and neovascularization). Finally, an evaluation of the capsule thickness detected around the discs was carried out by performing at least 10 thickness measurements in both the upper and lower margins of the capsule.

After the explant, the discs were examined, to assess: i) the occurrence of possible detachments, fracturing and/or fragments release during implantation (which is an indirect sign of possible nanotoxicity) - FEG-SEM (performed as described above); ii) the durability of the coatings, assessed by verifying its residual presence after 28 days implantation - EDS (Bruker probe coupled with the field emission gun scanning electron microscope); and iii) the maintenance of their antibacterial efficacy. Samples were cleaned in ethanol and water for 24 h, then observed as received, without any preparation, including fixation, embedding or metallization.

2.6.3. Systemic toxicity assessment with inductively coupled plasma mass spectrometry (ICP/MS)

The qualitative-quantitative analysis was performed according to IZSLER internal method for the research and determination of metals in foods of animal origin, by means of ICP/MS (Agilent 7700 ICP-MS equipped with an ASX-500 Series auto sampler). 1–2 mL of distilled water was added to about 3 g of weighted sample of organs. The samples were then subjected to a wet mineralization process entailing the addition of concentrated nitric acid and heating at 75 ± 10 °C overnight. The sample volume was adjusted to 20 mL by adding demineralized water and shacking vigorously. Part of the content was poured into 15 mL polystyrene tubes, then 1 mL of the obtained solution was diluted to 10 mL using a dilution solution (an aqueous solution of 2 % nitric acid with 0.5 % hydrochloric acid). For each series of analyses, a reagent blank was mineralized in the same way as the samples. In parallel with the evaluations, a reference sample is measured by ICP-MS to confirm that the results obtained with the study samples are the expected ones, respecting the measurement uncertainty ranges. The analyses were performed by MassHunter 4.2 Software (Agilent Technologies) and the quantitative determination was carried out on the most abundant and least interfered isotope. A calibration curve from 0,01–100 μg/mL was analyzed for each series of analyses: the correlation coefficient was equal to or >0.999 for each element subjected to analysis. A mixture of internal standards (each one having a concentration of 1 mg/mL) was infused continuously by a second way of entrance in ICP-MS to quantify the samples. The limit of determination (LoQ) was set at 0.002 mg/kg for all matrices. At the beginning of each measurement cycle, a tuning operation was carried out with a multi-element mixture to check the accuracy of the identification of the m/z ratio values and the accuracy of the instrument. Since the lower limit of application of the method is 0.002 mg/kg, both the absence of the metal and its presence in a concentration below this value is reported with <0.002 mg/kg (not detectable, ND).

2.7. Statistical analysis

Statistical analysis was performed using the SPSS/PC + Statistics TM 25.0 software package (SPSS Inc., Chicago, IL USA). After having verified the normal data distribution, microbiological, Alamar Blue and histomorphometric data were analyzed by using one-way ANOVA followed by *post-hoc* Scheffé test. Data are reported as Mean ± SD at a significance level of $p < 0.05$. All reported results are representative of at least three replicates. No statistical analysis has been performed for the data obtained from the application of the semi-quantitative evaluation score reported in Annex E of the UNI EN ISO 10993-6 standard, since the ISO standard provides an appropriate comparison framework.

3. Results

3.1. Coatings characterization

Coatings morphology is reported in Fig. 1. All coatings exhibited a nanostructured morphology, as they are composed of spherical aggregates of about 25 nm diameter, as already found by AFM and STM [42], which aggregate in clusters having diameters between 50 nm and 460 nm. No differences are noticed in the diameter of the grains or the aggregates when switching from 45 to 60 min deposition, but a general shift towards aggregates of larger dimensions.

Coatings appear uniform and no detachments are found in any area of the samples, including the edges (Fig. 2). Because of submicrometric thickness, they do not alter the microscale finishing of the implants, which is designed to ensure primary stability. The substrate itself was chosen to mimic the surface roughness and finishing of bone implants, and provided by the manufacturers after machining, so it shows several voids and irregularities, as it does in real prostheses. EDS data (supplementary material, Fig. S1) also confirmed the presence of Ag coatings in different areas and samples, and no significant variations were found among random zones in different samples. EDS maps (supplementary material, Fig. S2) also show that silver coatings uniformly cover the samples, without leaving bare areas.

Measuring of the mechanical properties and adhesion of the film was prevented by the thin thickness of the film and by the high mechanical properties of the metallic substrate.

3.2. In vitro cytotoxicity according to UNI EN ISO 10993: Part 5

Results of metabolic activity of BJ5ta cells cultured with coatings are presented in Fig. 3, expressed as a percentage of viable cells compared with negative control condition. Staining with Neutral red was also performed to visualize if silver nanocoatings induced microscopic changes in the morphological features of the fibroblast cells monolayer (Fig. 4).

Fig. 3 shows that BJ5ta cells were metabolically unaffected by nanostructured Ag-coatings as no significant differences were observed in Alamar Blue test among coatings and CTRM conditions, and no

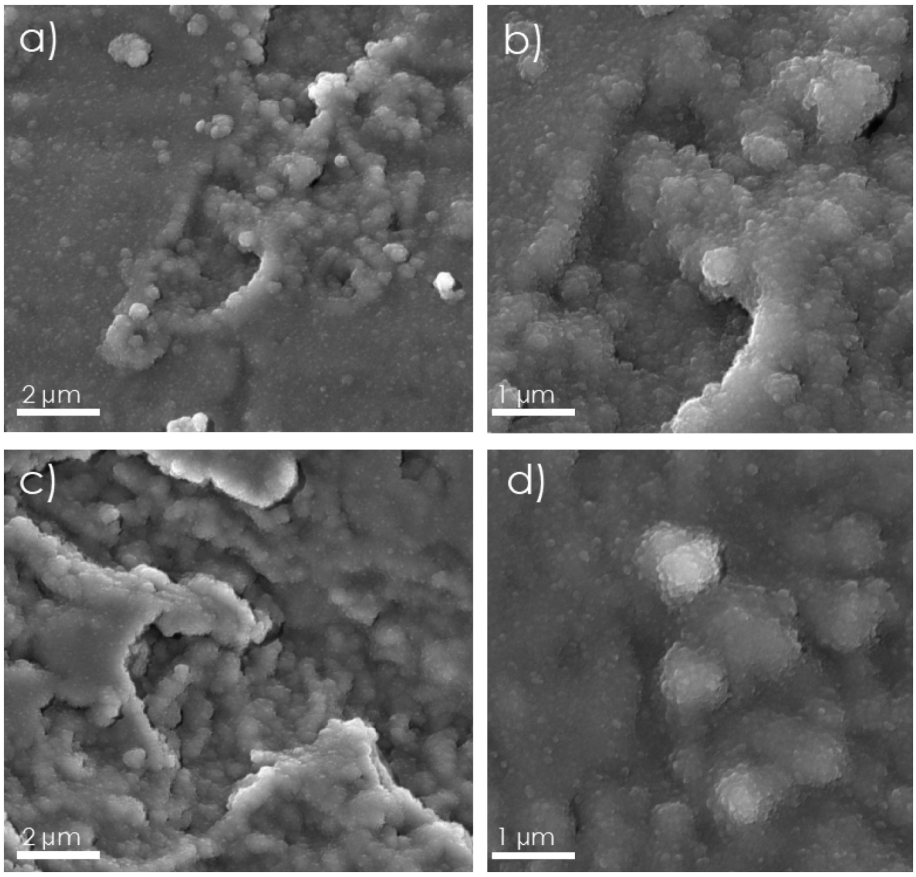

Fig. 1. Coatings morphology at 45 min (a and b) and 60 min deposition (c and d), as assessed by FEG-SEM.

significant LDH release was measured in the culture medium (*data not shown*) indicating that cells were not under metabolic anaerobic stress. Light microscopy investigation after Neutral Red staining showed no significant changes in cell morphology: cells appeared well stained with the dye and attached to the substrate. At the longest Ag deposition time (sample Ag60), some shrinkage was detected in some of the cells in direct contact with the coating, suggesting that deposition times longer than 60 min could induce an alteration or toxic effect (Fig. 4).

3.3. In vitro antibacterial and antibiofilm efficacy

Both *Escherichia coli* ATCC 8739 and *Staphylococcus aureus* ATCC 6538P strains perceived a significant antibacterial effect in their planktonic growth when incubated in the presence of silver coatings at all the tested deposition times (Fig. 5, Table 1). No growth of *E. coli* was observed in the presence of the three coatings compared to the control already after 2 h of incubation, meaning that no significant effect of the deposition time is observed. On the other hand, *S. aureus* perceived a delay in the planktonic growth in the presence of Ag30 and Ag45. In particular, Ag60 significantly inhibited *S. aureus* growth by causing almost a 3-log fold reduction in CFU/mL at 8 h incubation.

As for the planktonic growth, the antibiofilm capacity of the Ag-coated discs was higher against *E. coli* compared to *S. aureus*. The ability of *E. coli* cells to form biofilm on the Ag-coated discs was significantly lower than the control under all the conditions tested, showing a cell growth inhibition between 43 % and 53 %. On the other hand, a significant inhibition of the biofilm formation of *S. aureus* cells was observed only in the presence of Ag45 and Ag60, the latter showing a maximum inhibition value of 38 % (Fig. 6).

For many biomedical applications, efficacy against *E. coli* alone permits applicability, but *S. aureus* is the main responsible for orthopedic bacterial infections, so efficacy against this strain is also desired. Current results highlighted that an optimal efficacy against both strains was obtained only for the deposition times of 45 min and above. Therefore, Ag30 samples were not further characterized *in vivo*.

3.4. In vivo histocompatibility

All animals survived the implant surgery, no side effects or systemic complications were observed in the post-operative time and surgical wounds healed without complications. The body weight recorded during the experimental time showed an increase, with no differences being observed between the two groups at 4 weeks. Indeed, a weight starting from a mean value of 237 ± 3 g up to 477 ± 31 g was recorded for the Ag45 group, and 233 ± 6 g up to 449 ± 60 g was measured for the Ag60 group, at the end of the study. At the retrieval, all implants maintained their positioning at the subcutaneous tissue site and no macroscopic abnormalities were detected. Inspection of skin and tissue did not detect bluish-gray discoloration induced by silver deposition in skin micro vessels (argyria) (Fig. S3). Macroscopically, a thin, almost transparent, layer of connective tissue was detected, which covered all implanted discs and still allowed a clear view of the underlying material. There were no evident signs of necrosis or adipose tissue infiltration (Fig. S3B, C, D). After histological processing and hematoxylin/eosin staining, no accumulation of Ag-containing granules was detected either in the dermis or at the basement membrane level, and the tissues in direct contact with coatings revealed no signs of inflammation or severe immune reactions (Fig. 7). The panoramic vision clearly shows the histological appearance of normal rat skin. A cavity was clearly visible originally occupied by the discs, surrounded by a mature connective tissue capsule; the tissue responses for both nanostructured coatings and control were overall similar, as confirmed by the semi-quantitative score

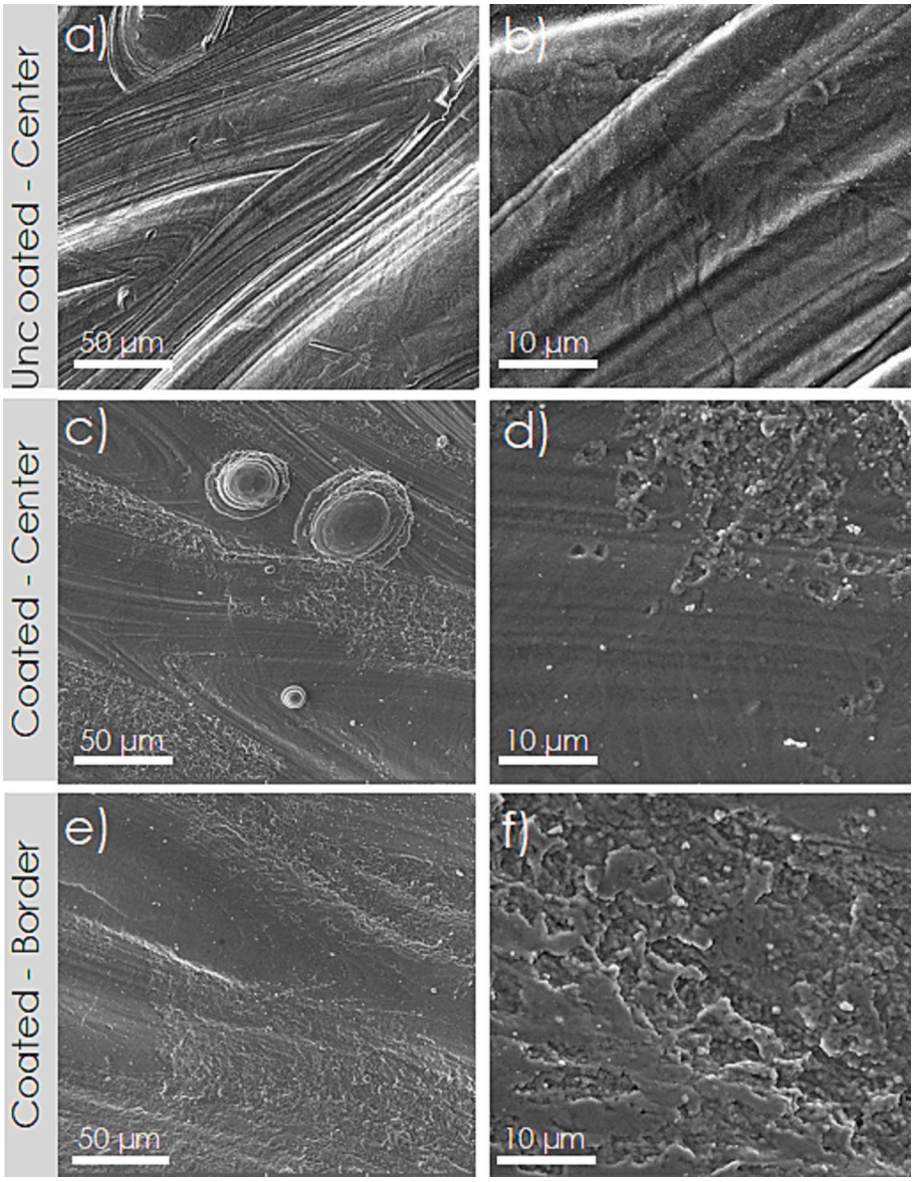

Fig. 2. Morphology of uncoated (a and b) and coated samples (Ag60) (c to f). No defects or detachments are noticed on either the samples center (c and d) or edge (e and f).

(Annex E UNI EN ISO 10993: 6) and can be categorized as causing "minimal or no reaction". The cellularity and number of macrophages and giant cells were similar among silver nanostructured coatings and controls. A negligible inflammatory cell response was detected. The degree of cellularity and neovascularization was similar for coated and uncoated devices. This data was also confirmed by the measure of connective tissue thickness: the statistical analysis showed that the mean thickness measured for the Ag45 was 31.0 ± 3.8 μm, which was significantly lower ($p < 0.05$) than that measured for Ag60 (43.0 ± 3.6 μm) and for the control (44.0 ± 3.0 μm). No difference was detected between Ag60 and control substrate.

At 4 weeks from implantation, Ag was still present on Ag45 (33 ± 29 wt%) and Ag60 (1.4 ± 1.2 wt%) discs as showed by SEM/EDS (Fig. 8). The presence of Ag showed high variability, depending on the tested area analyzed on the sample, indicating that significant dissolution occurred especially for Ag60.

3.5. Inductively coupled plasma mass spectrometry (ICP/MS)

The concentration of Ag in the different organs is reported in Table 2, according to their abundance in the analyzed samples. To the best of Authors' knowledge, few quantitative data are available about distribution and accumulation following the exposure derived from an implant coated with nanostructured coatings. Classical histopathology is affected by limitations given by the nanostructure and submicrometric thickness of the coatings, that make detachments and particles release not visible under optical/fluorescence microscopy, except for micro aggregates or macroscopically visible histological alterations. Hence, it is difficult to establish organ toxicity by only using this approach. Instead, ICP-MS has a very sensitive detectability threshold and permits to detect also traces of metals accumulated in the tissues.

Our data, acquired with this method, showed that in all the analyzed organs, Ag accumulation was very close or below the detectability threshold of ICP-MS (<0.002 mg/kg), apart from the brain in both animal groups (Ag45 and Ag60).

3.6. Antibacterial activity of retrieved Ag-coated discs after in vivo experiments

The antibacterial activity of nanostructured Ag-coated discs

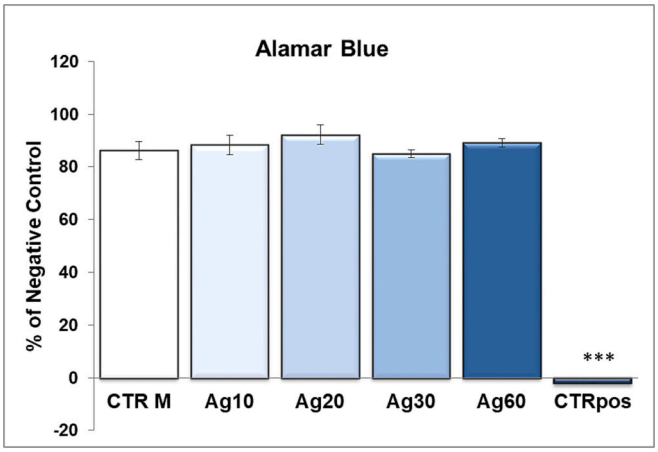

Fig. 3. Metabolic activity of BJ5ta fibroblast cell line cultured with silver nanostructured coatings with different deposition times: 10, 20, 30 and 60 min, corresponding to different nanofilm thicknesses, reported as % of negative control condition (cells cultured on the tissue culture plastic). All the values have been normalized for the values obtained for the CTRneg (BJ5ta cells not in contact with the tested coatings, but seeded onto polystyrene wells). Bars present the Mean ± SD obtained from three replicate materials. (CTRM refers to cells cultured in contact with the uncoated Ti_6Al_4V discs, while CTRpos refers to cells treated with a toxic agent (1 % phenol) dissolved in the culture medium). (***: CTRpos *vs* all conditions, $p < 0.001$).

retrieved at 4-weeks from surgery is shown in Fig. 9. Slight residual efficacy was present against both bacterial strains with a higher reduction of *E. coli* compared to *S. aureus*. For both strains the inhibition rate depended on the deposition time, being higher in the presence of Ag60. Moreover, the antibacterial activity was stronger and statistically significant against both strains at the first hours of growth and higher compared to the latest phases of the growth curve.

4. Discussion

Starting from a pure Ag target, nanostructured coatings have been obtained by the IJD technique, having a thickness that depends on deposition time [43]. In a previous study we investigated silver films deposited at three different thicknesses with nominal value of 50 (Ag20 and Ag30), 80 (Ag50), and 150 nm (Ag60). The images were obtained adopting Atomic Force Microscopy (AFM) in tapping mode at room temperature with an NT-MDT microscope equipped with silicon cantilever (NT-MDT Co., Moscow, Russia). Hence, although films thickness wasn't measured here since the high roughness of the substrate prevents a correct measuring on titanium alloys by AFM, we can expect similar thickness for our films. In the previous results, AFM was employed to assess the film's continuity with the substrate, the absence of particulate matter and the surface nanostructure. The images also revealed a uniformly smooth surface with nanometric roughness, featuring a scarcity of aggregates or outgrowths, except for clusters not exceeding a few tens of nanometers. Further magnification revealed a distribution of nearly-spherical grains, each a few tens of nanometers in diameter, with no significant variations with increasing film thickness. These data match those obtained here. Indeed, all coatings deposited for 30 min and above exhibit a highly uniform, nanostructured surface texture, and are composed of spherical aggregates, with Ag30 being the thinner coatings providing complete substrate coverage and absence of defects. Deposition times up to over 120 min are permitted without observing defects (data not shown), but some toxicity is observed over 60 min. Moreover, previous works on the metal functionalization of surfaces with IJD technology also highlighted that 30 to 60 min is the optimal range of deposition to obtain reliable and reproducible antibacterial activities [50,51]. For these reasons, all deposition times above 60 min or below 30 were discarded [43]. Importantly, our past results also show that, despite the significant impact on coatings thickness, deposition time does not significantly alter coatings surface morphology (RMS values are 2.2 ± 0.2 μm for Ag30 and 2.7 ± 0.3 μm for Ag60) [43]. This rough surface morphology guarantees a high specific surface, that results in high efficacy.

Based on the deposition time, the Ag nanocoatings showed different efficacy against the planktonic and biofilm growth of *E. coli* and *S. aureus* strains. For 45- and 60-min deposition, significant inhibition of planktonic growth of both strains was observed, together with an inhibition of biofilm formation of about 50 % in the presence of both Ag45 and Ag60 in *E. coli*, and of 30 % (Ag45) and 40 % (Ag60) in *S. aureus*. On the other hand, Ag30 significantly inhibited only *E. coli* in both planktonic and biofilm growths. This different response to Ag between *E. coli* and *S. aureus* is in agreement with literature data, being *E. coli* generally more sensitive to the metal nanocoating in both planktonic and biofilm growth conditions [52,53]. In line with this, Graziani et al. had previously observed the different antibacterial activity on these two species provided by an Ag-tricalcium phosphate (TCP) coating manufactured by IJD, by measuring the number of adherent cells (*i.e.*, the first step of the biofilm formation process) and observing 70 % inhibition of *E. coli* and 26 % inhibition of *S. aureus* cells compared to TCP without Ag coating. In another study from the current Authors [49], where silver films were used to functionalize electrospun patches for wound healing, data showed a higher effect for *S. aureus* compared to *E. coli*. Although preliminary, these results indicated that also the substrate to which the coating is applied plays a role in the antibacterial efficacy of the device. This different efficacy depends on either: (i) different morphology promoting/discouraging bacterial adhesion; (ii) different specific surface determining silver ions release; and (iii) the interaction between the substrate and the coating which determine the possible formation of interlayers and the coating tendency to crack and release particles. Silver toxic effect on bacterial cells are multiple, including enhancement of ROS production, inactivation of efflux systems, and physical damage of the bacterial envelope [54]. The different bacterial cell composition between gram-positive and gram-negative bacterial strains can contribute to the different toxic effect of metal coatings against *E. coli* and *S. aureus* as reported in previous studies [50,51]. Gram-negative strains possess inner and outer membrane with a periplasmic space in between, whereas *S. aureus* has a thick and robust monolayer mostly composed by peptidoglycan. These two envelopes can prevent the internalization of toxic compounds (like metals) in different ways, the first one mostly through the action of enzymes present in the periplasmic space, the second one thanks to the physical barrier represented by the peptidoglycan layer [54]. These differences can explain the distinct sensitivity observed in this study, making the gram-positive *S. aureus* being more efficient in the limitation of Ag internalization compared to the gram-negative *E. coli*.

Beyond the physicochemical and microbiological characteristics of coatings, the use of nanostructured Ag raises several questions regarding stability, release, distribution (particles detaching from the coating can cross biological barriers and enter circulation) and the balance between the antimicrobial properties and toxicity to tissue and organs, which represent one of the most heated and controversial points. Importantly, our coatings are designed to release Ag ions and not nanoparticles, but the release of the latter due to damage during implantation or due to progressive dissolution cannot be excluded *a priori*.

Literature data report that the toxicity of Ag nanoparticles is partly due to the size (in addition to shape, surface chemistry, topography and concentration) and that smaller particles can induce greater toxicity as reported, among the others, by Akter M, who summarized different *in vitro* studies on the size dependent effects of Ag-NPs on several cell lines [55]. In the present set-up, results obtained for cytotoxicity tests showed that BJ-5TA fibroblasts experienced a negligible change in cell metabolic activity for all deposition conditions after 72 h. These data demonstrated that nanostructured Ag films can eradicate some of

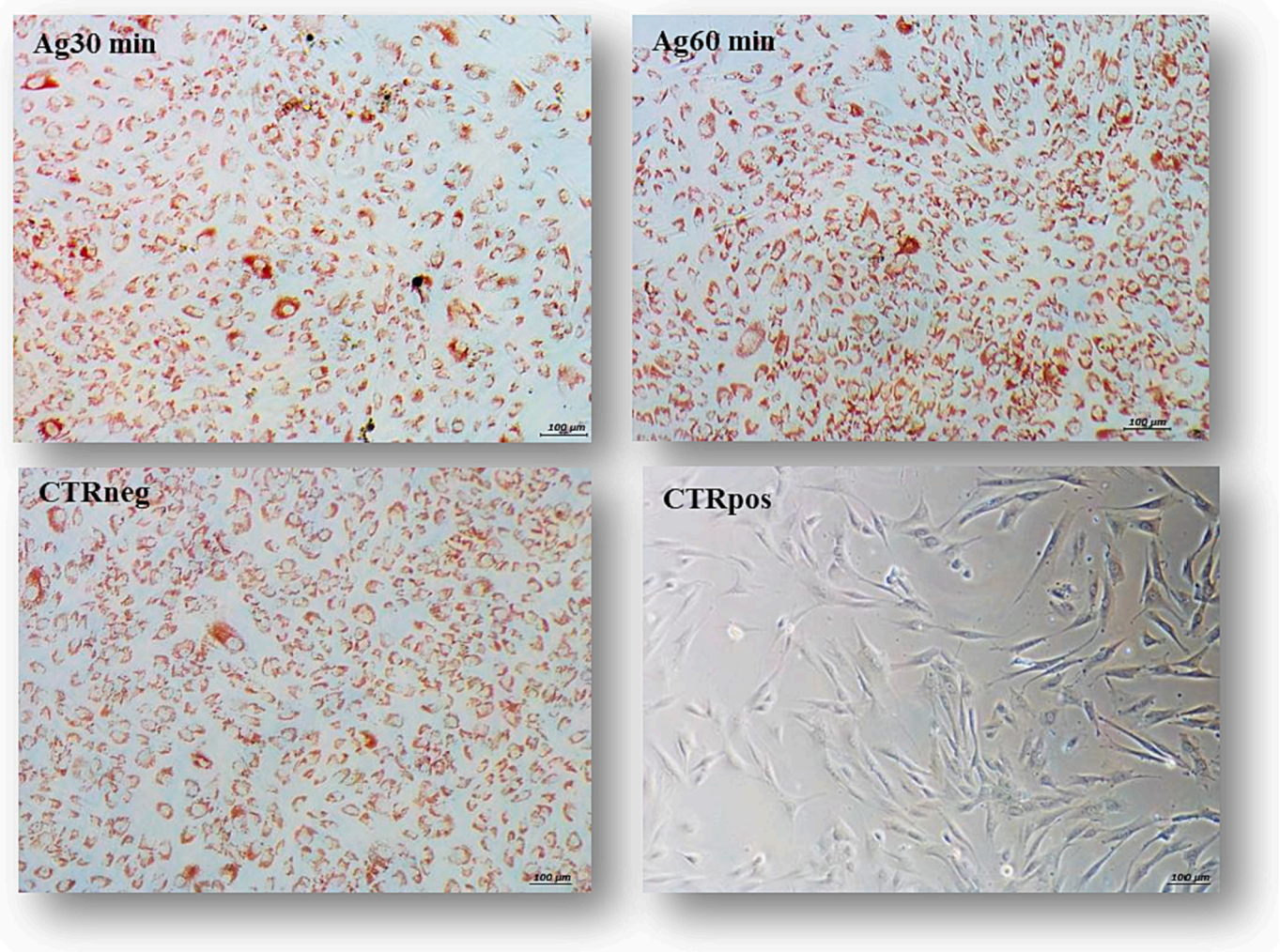

Fig. 4. Representative images of BJ5ta cells cultures stained with Neutral Red at the end of 72 h of culture under different conditions: cells in contact with Ag30 and Ag60 silver nanostructured coatings as well as cells in CTRneg condition (BJ5ta cells not in contact with the tested coatings, but seeded onto polystyrene wells) and CTRpos (BJ5ta cells not in contact with the tested coatings but treated with 1 % phenol solution). The images depict the post-staining condition with NR staining solution (Neutral Red) of the different cell's cultures. Neutral Red is a vital dye that is selectively internalized within lysosomal vesicles by only vital and metabolically active cells. Cells cultured with phenol (in the CTRpos condition) did not internalize the dye, suggesting a state of severe cellular distress, as evidenced by reduced cell confluence and number in the captured frame. Notably, no differences were observed between the two experimental coatings (Ag45 and Ag60) and the negative control condition (CTRneg condition). Images were acquired with Eclipse Tj-U inverted microscope (NIKON) at 10× magnification (scale bar:100 µm). (For interpretation of the references to colour in this figure legend, the reader is referred to the web version of this article.)

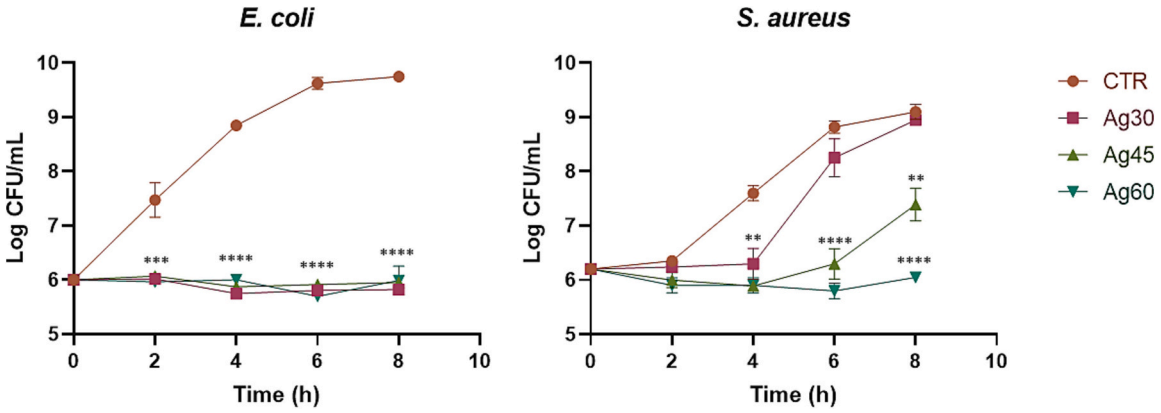

Fig. 5. Growth curves of planktonic cells of *Escherichia coli* ATCC® 8739™ and *Staphylococcus aureus* ATCC® 6538P™ (over 8 h of growth on LB medium) in the presence of Ag30, Ag45, and Ag60coated discs. The growth inhibition was evaluated by comparing the growth obtained at each time point in the presence of the different coated alloy discs with the presence of non-coated discs (CTR) (Mean ± SD, $n = 3$). (**: $p < 0.01$; ***: $p < 0.001$; ****: $p < 0.0005$).

Table 1
Antibacterial effect of Ag-coated discs on the bacterial growth in liquid medium at 2, 4, 6 and 8 h of incubation. The total number of Colony Forming Units (CFUs) per mL of culture is reported for each sample. The percentage of inhibition refers to the total number of viable CFUs per mL compared to the control experiment.

Strain	Time	Sample	Mean CFUs/mL	% inhibition *vs* CTR
E. coli	2 h	CTR	3.40e+07	–
		Ag30	1.05e+06	96.49
		Ag45	1.18e+06	96.09
		Ag60	9.25e+05	96.91
	4 h	CTR	7.11e+08	–
		Ag30	5.65e+05	99.92
		Ag45	7.47e+05	99.89
		Ag60	1.00e+06	99.86
	6 h	CTR	4.26e+09	–
		Ag30	6.40e+05	99.99
		Ag45	8.22e+05	99.98
		Ag60	5.01e+05	99.99
	8 h	CTR	5.65e+09	–
		Ag30	6.65e+05	99.99
		Ag45	9.00e+05	99.99
		Ag60	1.07e+06	99.99
S. aureus	2 h	CTR	2.26e+06	–
		Ag30	1.75e+06	22.82
		Ag45	1.02e+06	55.54
		Ag60	8.15e+05	64.56
	4 h	CTR	4.09e+07	–
		Ag30	2.21e+06	95.01
		Ag45	7.72e+05	98.06
		Ag60	8.15e+05	98.01
	6 h	CTR	6.72e+08	–
		Ag30	2.08e+08	73.10
		Ag45	2.21e+06	99.70
		Ag60	6.47e+05	99.91
	8 h	CTR	1.29e+09	–
		Ag30	8.97e+08	29.21
		Ag45	2.74e+07	98.06
		Ag60	1.13e+06	99.91

important pathogens with a low impact on cells activity in static conditions. The coating itself and clusters formation prevent the direct interaction between cells and very small sized aggregated with a lower effect from cellular point of view. Similar results have been obtained in a previous experience with IJD technique, adopted to realize an Ag-substituted tricalcium phosphate (Ag-TCP) challenged with mesenchymal stromal cells, for which viability and osteogenic differentiation were preserved [52]. However, data obtained here show that using silver alone permits a higher efficacy compared to the Ag-doped ceramic, especially against *S. aureus*, the main pathogen responsible for bacterial infection, while biocompatibility is not reduced.

In vitro results were confirmed by the *in vivo* tests. Four weeks after subcutaneous implant of nanostructured Ag-coating, all animals were healthy and fit and no undesirable side effects were observed, such as argyria. Biocompatibility was demonstrated for both coatings (Ag45 and Ag60) with no significant differences in overall tissue responses in term of inflammation and fibrosis compared to the control, which has the composition and surface finishing or standard orthopedic prostheses. This point represents a very important and breakthrough result.

In the wide panorama of antibacterial coatings, a key challenge is the realization of coatings with lasting effects *in vivo*, where the physiological microenvironment directly acts on them. The performed investigations demonstrated that Ag coatings were still present after 4 weeks from surgery, as demonstrated by SEM images and EDS, indicating a high durability. In addition, no defects or cracking were detected suggesting a progressive dissolution of the coating, without release of nanoparticles or fragments which could cause inflammation or unforeseen toxicity. Importantly, in this case, durability is not measured by ageing tests *in vitro* but directly *in vivo*, hence taking into consideration the whole complexity of the system. In addition, the presence of residual coating at 4 weeks after implantation and the absence of cracks, is an indirect sign of high adhesion to the substrate. Indeed, although the thin thickness of the film, together with the high roughness and mechanical properties of the substrate prevented us from measuring adhesion by scratch following ISO 20502:2016, still the coatings did sustain implantation and interaction with the surrounding tissues and fluids without cracking, as they would in the case of poorly adhesive films. EDS analysis revealed the presence of Ag for both coatings, even though a significantly higher concentration was measured for Ag45. Result comparable with those obtained for Ag45 were reported by Shevtson M. et al., who exploited a physical vapor deposition technique to deposit silver onto a porous titanium implant for direct skeletal attachment systems. At 1, 2 and 3 months after intramedullary insertion in a model of above-knee amputation, EDS showed a residual amount of Ag of 23.8 % [56]. In our case, the higher residual presence of Ag in Ag45, resulted in a lower antibacterial efficacy at 4 weeks, which was probably due to a progressive flattening of the coatings, which reduced its release, increasing its durability, but reducing efficacy. Hence, the Ag60 was inferred to be the best performing option [52].

Nanostructured materials are largely studied, in view of their improved performance including increased surface area, higher

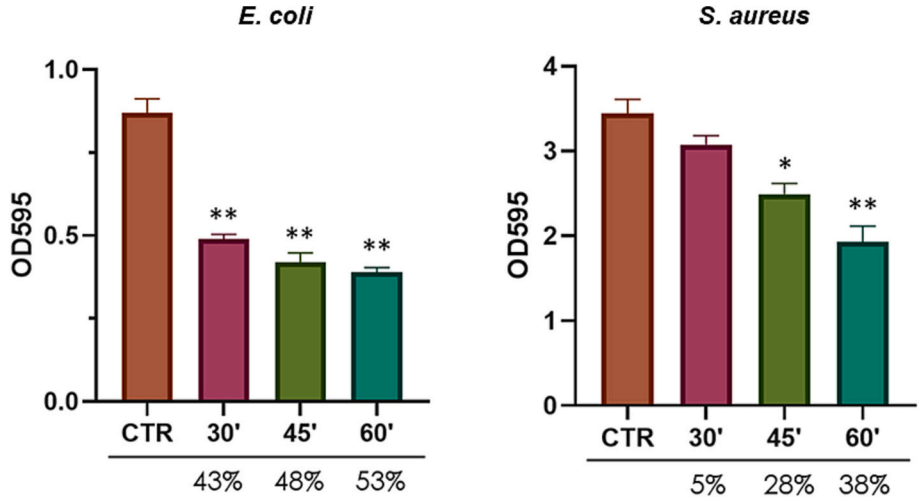

Fig. 6. Activity of Ag-coated titanium-aluminum-vanadium alloy discs against biofilm formation by *Escherichia coli* ATCC® 8739™ and *Staphylococcus aureus* ATCC® 6538P™. The reduction of absorbance (as compared to the control experiment, CTR, *i.e.*, inoculated growth medium with non-coated disc) is reported in percentage below each histogram (the mean value is reported below, while the SD is indicated in the graph, $n = 3$). (*: $p < 0.05$; **: $p < 0.01$).

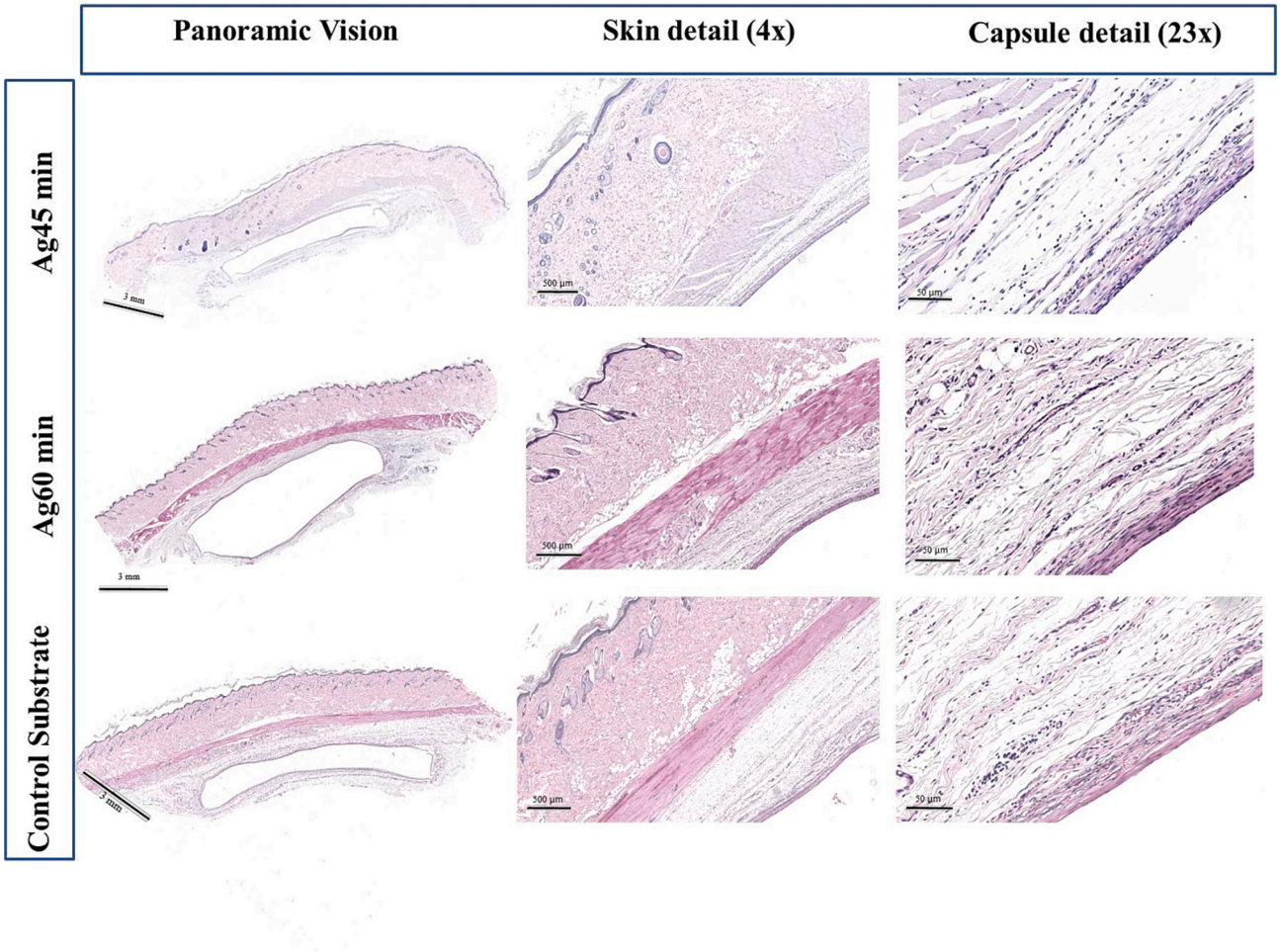

Fig. 7. Representative images of the subcutaneous implant sites. The images on the left showed a panoramic view of the entire skin biopsy in which a central lumen corresponding to the original implant site is visible. In the central column a major magnification of skin anatomic composition is reported while in right column it was provided a histological detail of the connective tissue formed around the implant. All histological sections were stained with Hematoxylin-Eosin and acquired with the Aperio Scanscope digital scanner. 0.6× magnification (scale bar = 3 mm) for the left images, 4× magnification (scale bar = 500 µm) for the central column and 23× for the right column (scale bar = 50 µm).

reactivity, and interaction with biological cues. However, the nanostructure raises questions related to safety and toxicity, since nanoparticles in certain size ranges, as well as the eventually released ions (such as Ag^{3+}), are highly mobile and can cross various biological barriers, enter circulation and become systemically available [57,58]. Therefore, nanosafety is a crucial aspect connected to the study of nanomaterials, and in last years, the number of papers focusing on the biodistribution and toxicity of nanoparticles significantly increased, taking into account the main routes of exposure represented by ingestion, inhalation and systemic (intraperitoneal or intravenous) injection [57]. In this scenario, despite the development and research of a wide variety of new Ag-based nanostructured coatings, very few studies assessed the accumulation and biodistribution of Ag derived from an implanted device, which represents therefore a neglected field of investigation, also considering the actual use of Ag coatings in several clinical and daily situations [59]. At the same time, also the interaction of Ag nanoparticles with other materials is still poorly investigated: nanocoatings interact with the substrate materials in a peculiar microenvironment represented by biological tissues (in this case bone) [60]. For our coatings, the Ag amounts quantified by ICP-MS were below the detectability threshold of the instrument for almost all the investigated organs (Supplementary Table 1), except for the brain, where the highest Ag concentration was measured. As previously mentioned, the administration route, dosage, and nanoparticle characteristics also affect the rate and methods of elimination. *In vivo* data from the literature suggest that AgNPs and Ag + ions are eliminated from most organs within 17 days to four months after the recovery period, following subacute inhalation, intravenous administration, and oral ingestion. Silver can be excreted through urine and feces (biliary excretion) after intravenous and subcutaneous administrations, thus providing a possible explanation for the lack of significant silver presence in the majority of our investigated organs [61,62]. Regarding silver presence in the brain, these data might raise concerns, as it is reported that Ag nanoparticles are able to penetrate the BBB and to accumulate in different areas [63]. In the brain, this metal can cause neurotoxicity, even if no consensus exists about the toxic level threshold that depends on several parameters (shape, dimension, surface charge, coating agent, dosage, and oxidation state). However, here, all the detected values (including those obtained in brain) are below the limits established by the EFSA (European Food Safety Authority), which limits the exposure derived from Ag ions in materials in contact with food, setting a threshold for Ag nanoparticles of 50 µg Ag/kg food. This threshold was defined considering a "*NOAEL (no observed adverse effect level) for human of 0.39 mg/person per day (6.5 µg/kg body weight/day, considering an adult of 60 kg bw)*" for silver exposure, defined by World Health Organization [64]. In addition, WHO fixed a limit of 0.1 mg/L as the silver levels which can be tolerated in drinking water [65]. Again, EFSA recommends not exceedingly globally 0.05 mg/L and 0.05 mg/kg in water and food silver content, respectively

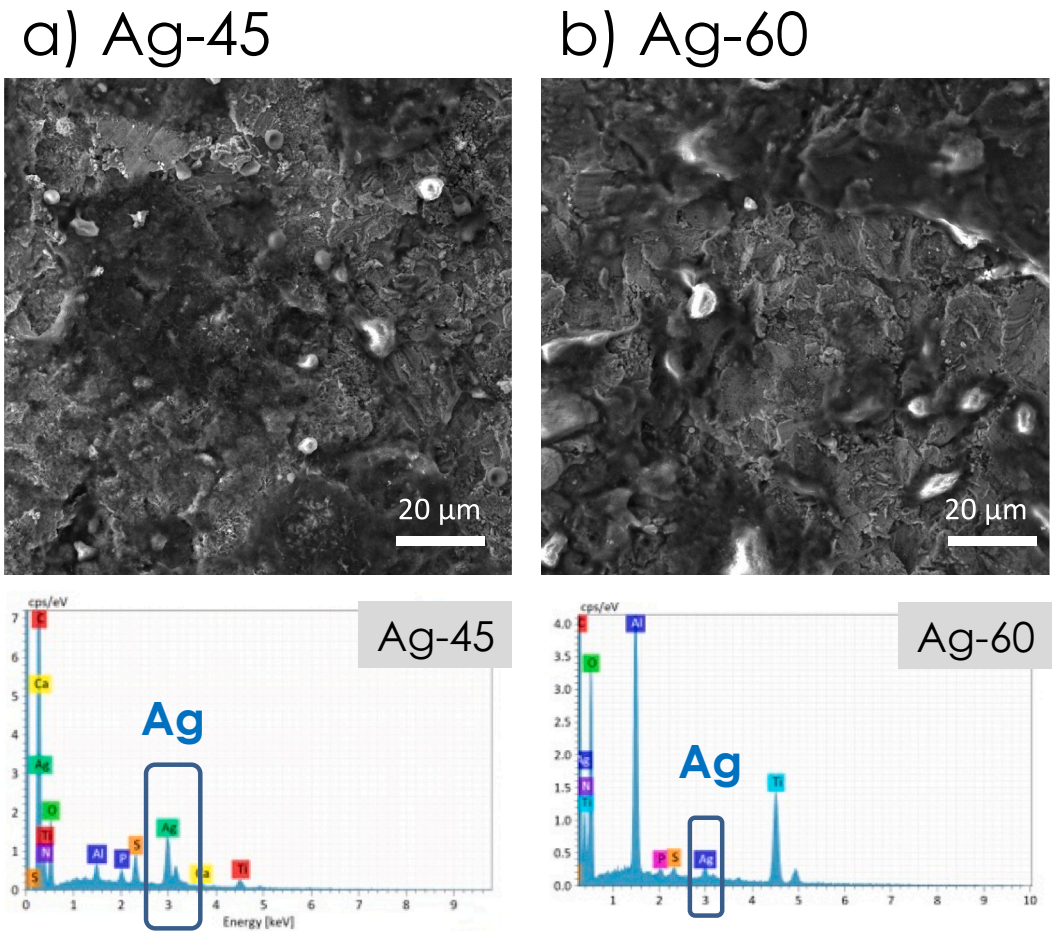

Fig. 8. SEM/EDS of samples Ag45 (a) and Ag60 (b) after explant. Peak relative to silver is in the blue box. (For interpretation of the references to colour in this figure legend, the reader is referred to the web version of this article.)

Table 2
Mean concentrations of silver in the different organs, as detected with ICP-MS technique. Data are reported as mg/kg ($n = 5$).

	Ag45 (n = 5)	Ag60 (n = 5)
BLOOD	0.002 ± 0.000	0.003 ± 0.001
HEART	0.002 ± 0.000	0.002 ± 0.000
SPLEEN	0.002 ± 0.000	0.003 ± 0.001
LIVER	0.003 ± 0.001	0.004 ± 0.001
BRAIN	0.010 ± 0.003	0.014 ± 0.005
KIDNEY	0.004 ± 0.001	0.005 ± 0.001
LUNG	0.002 ± 0.001	0.003 ± 0.001

[66]. Finally, in our case, it is not possible to define with the adopted methodology, if the detected value derive from brain endothelial cells or from brain tissues, that would indicate a BBB passage of nanoparticles or more probably of Ag ions [67,68].

Specifically, regarding Ag accumulation in brain, it is difficult to evaluate our data in comparison to the Literature, since differences in set-ups, routes of exposure (oral administration, intravenous or subcutaneous injection), formulation, size, analytical methods and their thresholds as well as animal models (species, strain, age, housing and inter-animal differences) hamper the possibility to compare data of different studies [61,63,69]. Despite this, some considerations for the values obtained, especially for those related to the brain, might be derived. Very few information is available from *in vivo* studies on silver/nanosilver for what regards tissue and/or organ biodistribution after its use as coating for implanted devices. In fact, only one *in vivo* study was found. Tsukamoto M. et al., evaluated the sub-acute toxicity of thermal sprayed Ag/HA coated titanium with two different Ag concentrations (2 % and 50 %) after bone implant in rat tibiae, in comparison to HA coating without Ag [70]. They performed ICP-MS analysis to detect Ag concentration in serum and organs (brain, liver, kidney and spleen) at different time points including 4 weeks after bone implant. A silver concentration of 0.02 µg/g was detected in the brain, which corresponds exactly to highest value detected in the current study (0.02 mg/kg). This silver concentration was found in the animal implanted with the 2 % Ag/HA coating but also in the control group (HA coating only without Ag coating). In their study, the Ag concentration in brain detected at 4 weeks was even higher for the group that received the implants with a higher silver amount (50 % Ag/HA, resulting in 0.05 µg/of silver accumulated in the target organ) [70]. Subsequent studies carried out by the same group with a higher concentration of silver (3 % Ag-HA) have shown the capability of this coating to inhibit bacterial adhesion and growth, enhancement of osteoconductivity in *in vivo* model and biological safety [71].

Most of the studies regarding Ag coatings focused only on metal serum levels, reporting a very wide range of results, depending on the multiple experimental variables. Serum values were used since threshold values are established that connect serum levels with toxic phenomena (*i.e.*, argyrosis, leukopenia, damage to liver and kidney function). More into detail, toxic phenomena result from blood concentrations of about 300 ppb, while silver below 200 ppb is to be considered normal for humans [72].

The topic of evaluation of silver accumulation in target organs and of setting a threshold of toxicity is an open challenge and has great importance. Indeed, to date, about 30 % of the products on the market, such as textiles, cosmetics, medical devices, food contact materials, and

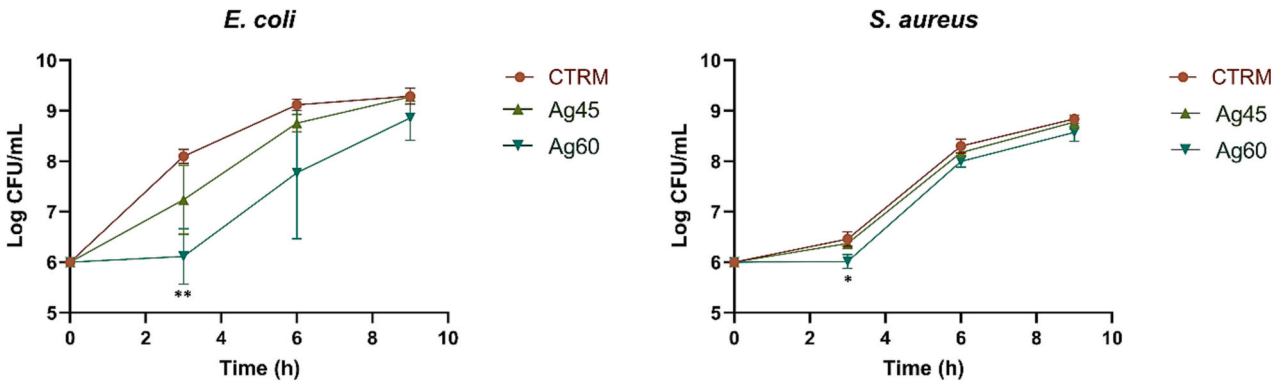

Fig. 9. Activity of retrieved nanostructured Ag-coated discs against the planktonic growth of *Escherichia coli* ATCC® 8739™ and *Staphylococcus aureus* ATCC® 6538P™ compared to the control experiments (CTR, inoculated growth medium with non-coated disc) (Mean ± SD, n = 5) (test: *: $p < 0.05$; **: $p < 0.01$).

even some food categories and water, have Ag as an ingredient or contaminant in different forms, including nanoparticles. This exponential growth and use of Ag even as nanoparticles is not counterbalanced by comprehensive scientific investigations about the potential toxic effects, which affect not only silver but also other metals [73]. For this reason, our studies on Ag biodistribution in organs are presented as a starting point for evaluating nanotoxicity in this new emerging technology, IJD, and to set a benchmark for evaluation of similar techniques, such as magnetron sputtering and pulsed laser deposition.

Despite very promising results, the study had some limitations. One is certainly represented by the absence of the investigation of Ag localization at a tissue level: it must be clarified whether the values especially those derived from brain belongs to blockage exerted from endothelial cells or from brain tissue and in this latter scenario would be important to understand in which tissues Ag is mainly localized. Furthermore, an Ag counterpart without nano-structure can be tested as well as biochemical parameters, which would help further defining the toxicity profile.

The overall *in vitro* and *in vivo* results show the efficacy and cytocompatibility of nanostructured Ag-coatings obtained by IJD, making them suitable candidates for antibacterial implant functionalization, to reduce the onset of infection. Despite the encouraging results, also from the nanosafety point of view, further studies are in progress, adopting experimental set-ups which consider implants coated with silver nanostructured coatings and nanoparticles. These studies will allow to deeply investigate and characterize the biodistribution of nanoparticles or ions deriving from this route of exposure, as well as the interaction of Ag with material substrate which represents a possible way for its transformation and can act on its biodistribution. In addition, to progress towards future clinical application, *in vivo* evaluation of antibacterial efficacy is also needed to investigated silver nanocoatings action in a more representative microenvironment.

5. Conclusions

In the global scenario of strategies to prevent infection deriving from implanted devices, the present paper reports the preclinical characterization, from *vitro* to *vivo*, of a new silver nanostructured coating realized by IJD. Adopting this technique, the Authors had already manufactured nanostructured thin coatings with anti-wear and pro-osseointegrative properties starting from a ceramic target: they provided the feasibility of this technique to obtain nanostructured thin films at room temperature onto different substrates (bioglass, zirconia, hydroxyapatite on metal and polymers), with a fine control over surface morphology and composition. Starting from this acquired knowledge with IJD, a nanostructured Ag-coating for metal substrate was realized and characterized for a possible exploitation in the field of antimicrobial nanotechnology since a wide antimicrobial and antiviral efficacy is recognized for silver, which made this material one of the most investigated inorganic metals for biomedical applications [74].

Data obtained showed that the films have high antibacterial and antibiofilm efficacy against gram-positive and gram-negative bacterial strains and do not show cytotoxic effects. Efficacy depends on deposition parameters and on the duration of the deposition, which also determines films thickness. Once the thickness is optimized, complete inhibition of bacterial viability is obtained for both strains, as well as a significant reduction in their capability to adhere to the substrate. Importantly, efficacy is retained for over 4 week, after implantation in animal models. Coatings showed a nanostructured surface morphology that permitted to avoid interference with viability and metabolic activity of host cells and, indeed, biocompatibility is verified *in vitro* and *in vivo*. Hence, once optimal parameters are set, antibacterial efficacy against *S. aureus* and *E. coli* can be merged with the encouraging results about distribution and nanotoxicity, indicating that the developed coatings are promising for application in orthopedic prostheses.

Fundings

The research was partially funded by the METACOS Project "Trattamento delle amputazioni mediante osteointegrazione" granted by INAIL-Istituto Nazionale per l'Assicurazione contro gli Infortuni sul Lavoro.

CRediT authorship contribution statement

Gabriela Graziani: Writing – review & editing, Writing – original draft, Visualization, Validation, Supervision, Project administration, Methodology, Investigation, Formal analysis, Data curation, Conceptualization. **Daniele Ghezzi:** Writing – review & editing, Writing – original draft, Visualization, Validation, Supervision, Project administration, Methodology, Investigation, Formal analysis, Data curation, Conceptualization. **Marco Boi:** Writing – review & editing, Methodology, Investigation, Formal analysis, Data curation. **Nicola Baldini:** Writing – review & editing, Supervision. **Enrico Sassoni:** Writing – review & editing, Validation, Resources, Methodology, Investigation, Formal analysis, Data curation. **Martina Cappelletti:** Writing – review & editing, Validation, Resources, Methodology, Investigation, Formal analysis, Data curation. **Giorgio Fedrizzi:** Writing – review & editing, Methodology, Investigation, Formal analysis, Data curation. **Melania Maglio:** Writing – review & editing, Validation, Methodology, Investigation, Formal analysis, Data curation. **Francesca Salamanna:** Writing – review & editing, Validation, Methodology, Investigation, Formal analysis, Data curation. **Matilde Tschon:** Writing – review & editing, Validation, Methodology, Investigation, Formal analysis, Data curation. **Lucia Martini:** Supervision, Methodology, Investigation. **Stefano Zaffagnini:** Writing – review & editing,

Resources, Project administration. **Milena Fini:** Writing – review & editing, Supervision, Resources, Project administration, Funding acquisition, Conceptualization. **Maria Sartori:** Writing – review & editing, Writing – original draft, Visualization, Validation, Supervision, Project administration, Methodology, Investigation, Formal analysis, Data curation, Conceptualization.

Declaration of competing interest

The authors declare that they have no known competing financial interests or personal relationships that could have appeared to influence the work reported in this paper.

Data availability

The data that support the findings of this study are partly available within the article supplementary materials. The others are available from the corresponding author, [Gabriela Graziani], upon reasonable request.

Appendix A. Supplementary data

Supplementary data to this article can be found online at https://doi.org/10.1016/j.bioadv.2024.213815.

References

[1] N.C.T. Dadi, B. Radochová, J. Vargová, H. Bujdáková, Impact of healthcare-associated infections connected to medical devices-an update, Microorganisms 9 (11) (2021) 2332.

[2] European Centre for Disease Prevention and Control, Healthcare-associated infections: surgical site infections Annual Epidemiological Report for 2017, Available from: https://www.ecdc.europa.eu/en/publications-data/healthcare-associated-infections-surgical-site-infections-annual-1.

[3] M. Sartori, V. Borsari, M. Maglio, S. Brogini, L. Bragonzoni, S. Zaffagnini, M. Fini, Skin adhesion to the percutaneous component of direct bone anchored systems: systematic review on preclinical approaches and biomaterials, Biomater. Sci. 9 (21) (2021) 7008–7023.

[4] A. Devlin-Mullin, N.M. Todd, Z. Golrokhi, H. Geng, M.A. Konerding, N.G. Ternan, J.A. Hunt, R.J. Potter, C. Sutcliffe, E. Jones, P.D. Lee, C.A. Mitchell, Atomic layer deposition of a silver nanolayer on advanced titanium orthopedic implants inhibits bacterial colonization and supports vascularized de novo bone ingrowth, Adv. Healthc. Mater. 6 (11) (2017).

[5] L. Pirisi, F. Pennestrì, M. Viganò, G. Banfi, Prevalence and burden of orthopaedic implantable-device infections in Italy: a hospital-based national study, BMC Infect. Dis. 20 (1) (2020) 337.

[6] B. Li, T.J. Webster, Bacteria antibiotic resistance: new challenges and opportunities for implant-associated orthopedic infections, J. Orthop. Res. 36 (1) (2018) 22–32.

[7] W.R. Fordham, S. Redmond, A. Westerland, E.G. Cortes, C. Walker, C. Gallagher, C. J. Medina, F. Waecther, C. Lunk, R.F. Ostrume, G.A. Caputo, J.D. Hettinger, R. R. Krchnavek, Silver as a bactericidal coating for biomedical implants, Surf. Coat. Technol. 253 (2014) 52–57.

[8] C. Mohiti-Asli, T. Molina, B. Diteepeng, B. Pourdeyhimi, E.G. Loboa, Evaluation of silver ion-releasing scaffolds in a 3D coculture system of MRSA and human adipose-derived stem cells for their potential use in treatment or prevention of osteomyelitis, Tissue Eng. Part A 22 (21–22) (2016) 1258–1263.

[9] F. Paladini, M. Pollini, A. Talà, P. Alifano, A. Sannino, Efficacy of silver treated catheters for haemodialysis in preventing bacterial adhesion, J. Mater. Sci. Mater. Med. 23 (8) (2012) 1983–1990.

[10] V. Alt, Antimicrobial coated implants in trauma and orthopaedics-a clinical review and risk-benefit analysis, Injury 48 (2017) 599–607.

[11] Z. Wu, B. Chan, J. Low, J.J.H. Chu, H.W.D. Hey, A. Tay, Microbial resistance to nanotechnologies: an important but understudied consideration using antimicrobial nanotechnologies in orthopaedic implants, Bioact. Mater. 16 (2022) 249–270.

[12] E. Zhang, X. Zhao, J. Hu, R. Wang, S. Fu, G. Quin, Antibacterial metals and alloys for potential biomedical implants, Bioact. Mater. 6 (8) (2021) 2569–2612.

[13] A. Sathiyaseelan, K. Saravanakumar, M.H. Wang, Bimetallic silver-platinum (AgPt) nanoparticles and chitosan fabricated cotton gauze for enhanced antimicrobial and wound healing applications, Int. J. Biol. Macromol. 220 (2022) 1556–1569.

[14] M. Gosau, M. Haupt, S. Thude, M. Strowitzki, B. Schminke, R. Buergers, Antimicrobial effect and biocompatibility of novel metallic nanocrystalline implant coatings, J. Biomed. Mater. Res. Part B 104B (2016) (2016) 1571–1579.

[15] D.P. Dowling, K. Donnelly, M.L. McConnell, R. Eloy, M.N. Arnaud, Deposition of anti-bacterial silver coatings on polymeric substrates, Thin Solid Films 398–399 (2001) 602–606.

[16] E.M. Sussman, B.J. Casey, D. Dutta, B.J. Dair, Different cytotoxicity responses to antimicrobial nanosilver coatings when comparing extract-based and direct-contact assays, J. Appl. Toxicol. 35 (2015) 631–639.

[17] H. Cao, X. Liu, F. Meng, P.K. Chu, Biological actions of silver nanoparticles embedded in titanium controlled by micro-galvanic effects, Biomaterials 32 (2011) 693e705.

[18] S. Qiao, H. Cao, X. Zhao, H. Lo, L. Zhuang, Y. Gu, J. Shi, X. Liu, H. Lai, Ag-plasma modification enhances bone apposition around titanium dental implants: an animal study in Labrador dogs, Int. J. Nanomedicine 10 (2015) 653–664.

[19] C. Moseke, U. Gbureck, P. Elter, P. Drechsler, A. Zoll, R. Thull, A. Ewald, Hard implant coatings with antimicrobial properties, J. Mater. Sci. Mater. Med. 22 (12) (2011) 2711–2720.

[20] S. Spange, A. Pfuch, C. Wiegand, O. Beier, U.C. Hipler, B. Grünler, Atmospheric pressure plasma CVD as a tool to functionalise wound dressings, J. Mater. Sci. Mater. Med. 26 (2) (2015) 76.

[21] R. Xu, X. Yang, J. Jiang, P. Li, X. Zhang, G. Wu, P.K. Chu, Effects of silver plasma immersion ion implantation on the surface characteristics and cytocompatibility of titanium nitride films, Surf. Coat. Technol. 279 (2015) 166–170.

[22] M. Bosetti, A. Massè, E. Tobin, M. Cannas, Silver coated materials for external fixation devices: in vitro biocompatibility and genotoxicity, Biomaterials 23 (3) (2002) 887–892.

[23] E.P. Ivanova, J. Hasan, V.K. Truong, J.Y. Wang, M. Raveggi, C. Fluke, R. J. Crawford, The influence of nanoscopically thin silver films on bacterial viability and attachment, Appl. Microbiol. Biotechnol. 91 (4) (2011) 1149–1157.

[24] R. Barnbauer, P. Mestres, R. Schiel, J. Klinkrnann, P., Sioshansi surface-treated catheters with ion beam-based process evaluation in rats, Artif. Organs 21 (9) (1997) 1039–1041.

[25] R. Bambauer, R. Schiel, C. Bambauer, R. Latza, Surface-treated versus untreated large-bore catheters as vascular access in hemodialysis and apheresis treatments, Int. J. Nephrol. 2012 (2012) 956136.

[26] I.N. Mihailescu, D. Bociaga, G. Socol, G.E. Stan, M.C. Chifiriuc, C. Bleotu, M. A. Husanu, G. Popescu-Pelin, L. Duta, C.R. Luculescu, I. Negut, C. Hapenciuc, C. Besleaga, I. Zgura, F. Miculescu, Fabrication of antimicrobial silver-doped carbon structures by combinatorial pulsed laser deposition, Int. J. Pharm. 515 (1–2) (2016) 592–606.

[27] G. Benetti, E. Cavaliere, A. Canteri, G. Landini, G.M. Rossolini, L. Pallecchi, M. Chiodi, M.J. Van Bael, N. Winckelmans, S. Bals, L. Gavioli, Direct synthesis of antimicrobial coatings based on tailored bi-elemental nanoparticles, APL Mater. 5 (2017) 036105.

[28] L.L. Woodyard, T.L. Bowersock, J.J. Turek, G.P. McCabe, J. DeFord, A comparison of the effects of several silver-treated intravenous catheters on the survival of staphylococci in suspension and their adhesion to the catheter surface, J. Control. Release 40 (1–2) (1996) 23–30.

[29] X. Zhang, H. Wang, J. Li, X. He, R. Hang, Y. Yang, B. Tang, The fabrication of ag-containing hierarchical micro/nano-structure on titanium and its antibacterial activity, Mater. Lett. 193 (2017) 97–100.

[30] D. Bociaga, P. Komorowski, D. Batory, W. Szymanski, A. Olejnik, K. Jastrzebski, W. Jakubowsk, Silver-doped nanocomposite carbon coatings (ag-DLC) for biomedical applications – physiochemical and biological evaluation, Appl. Surf. Sci. 355 (1–2) (2015) 388–397.

[31] A. Gao, R. Hang, P.K. Chua, Recent advances in anti-infection surfaces fabricated on biomedical implants by plasma-based technology, Surf. Coat. Technol. 312 (2017) 2–6.

[32] C. Qi, A.V. Rogachev, D.V. Tapal'skii, M.A. Yarmolenko, A.A. Rogachev, X. Jiang, E.V. Koshanskaya, A.S. Vorontsov, Nanocomposite coatings for implants protection from microbial colonization: formation features, structure, and properties, Surf. Coat. Technol. 315 (2017) 350–358.

[33] M. Fosca, A. Streza, I.V. Antoniac, G. Vadalà, J.V. Rau, Ion-doped calcium phosphates-based coatings with antibacterial properties, J. Funct. Biomater. 14 (5) (2023) 250.

[34] J. Davenas, P. Thévenard, F. Philippe, M.N. Arnaud, Surface implantation treatments to prevent infection complications inshort term devices, Biomol. Eng. 19 (2–6) (2002) 263–268.

[35] T. Kocourek, M. Jelínek, J. Mikšovský, K. Jurek, M. Weiserová, Silver doped metal layers for medical applications, J. Phys. Conf. Ser. 497 (2014) 012021.

[36] X. Chen, J. Zhou, Y. Qian, L.Z. Zhao, Antibacterial coatings on orthopaedic implants, Mater. Today Bio 19 (2023) 100586.

[37] J.K. Pandey, R.K. Swarnkar, K.K. Soumya, P. Dwivedi, M.K. Singh, S. Sundaram, R. Gopal, Silver nanoparticles synthesized by pulsed laser ablation: as a potent antibacterial agent for human enteropathogenic gram-positive and gram-negative bacterial strains, Appl. Biochem. Biotechnol. 174 (3) (2014) 1021–1031.

[38] P.N. Catalano, M. Pezzoni, C. Costa, G.J.A.A. Soler-Illia, M.G. Bellino, M. F. Desimone, Optically transparent silver-loaded mesoporous thin film coating with long-lasting antibacterial activity, Microporous Mesoporous Mater. 236 (2016) 158–166.

[39] J. Schmolders, S. Koob, P. Schepers, P.H. Pennekamp, S. Gravius, D.C. Wirtz, R. Placzek, A.C. Strauss, Lower limb reconstruction in tumor patients using modular silver-coated megaprostheses with regard to perimegaprosthetic joint infection: a case series, including 100 patients and review of the literature, Arch. Orthop. Trauma Surg. 137 (2) (2017) 149–153.

[40] C.K. Wei, S.J. Ding, Dual-functional bone implants with antibacterial ability and osteogenic activity, J. Mater. Chem. B 5 (10) (2017) 1943–1953.

[41] S. Li, T. Zhu, J. Huang, Q. Guo, G. Chen, Y. Lai, Durable antibacterial and UV-protective ag/TiO2@ fabrics for sustainable biomedical application, Int. J. Nanomedicine 12 (2017) 2593–2606.

[42] G. Graziani, M. Berni, A. Gambardella, M. De Carolis, M.C. Maltarello, M. Boi, G. Carnevale, M. Bianchi, Fabrication and characterization of biomimetic hydroxyapatite thin films for bone implants by direct ablation of a biogenic source, Mater. Sci. Eng. C Mater. Biol. Appl. 99 (2019) 853–862.
[43] A. Gambardella, M. Berni, G. Graziani, A. Kovtun, F. Liscio, A. Russo, A. Visani, M. Bianchi, Nanostructured Ag thin films deposited by pulsed electron ablation, Appl. Surf. Sci. 475 (2019) 917–925.
[44] D. Bellucci, M. Bianchi, G. Graziani, A. Gambardella, M. Berni, A. Russo, V. Cannillo, Pulsed electron deposition of nanostructured bioactive glass coatings for biomedical applications, Ceram. Int. 43 (17) (2017) 15862–15867.
[45] M. Bianchi, A. Gambardella, G. Graziani, F. Liscio, M.C. Maltarello, M. Boi, M. Berni, D. Bellucci, G. Marchiori, F. Valle, A. Russo, M. Marcacci, Plasma-assisted deposition of bone apatite-like thin films from natural apatite, Mater. Lett. 199 (2017) 32–36.
[46] M. Bianchi, L. Degli Esposti, A. Ballardini, F. Liscio, M. Berni, A. Gambardella, S.C. G. Leeuwenburgh, S. Sprio, A. Tampieri, M. Iafisco, Strontium doped calcium phosphate coatings on poly(etheretherketone) (PEEK) by pulsed electron deposition, Surf. Coat. Technol. 319 (2017) 191–199.
[47] M. Bianchi, A. Gambardella, M. Berni, S. Panseri, M. Montesi, N. Lopomo, A. Tampieri, M. Marcacci, A. Russo, Surface morphology, tribological properties and in vitro biocompatibility of nanostructured zirconia thin films, J. Mater. Sci. Mater. Med. 27 (5) (2016) 96.
[48] G. Graziani, D. Ghezzi, F. Nudelman, E. Sassoni, F. Laidlaw, M. Cappelletti, M. Boi, G. Borciani, S. Milita, M. Bianchi, N. Baldini, G. Falini, A natural biogenic fluorapatite as a new biomaterial for orthopaedics and dentistry: antibacterial activity of lingula seashell and its use for nanostructured biomimetic coatings, J. Mater. Chem. B (2024).
[49] G. Pagnotta, G. Graziani, N. Baldini, A. Maso, M.L. Focarete, M. Berni, F. Biscarini, M. Bianchi, C. Gualandi, Nanodecoration of electrospun polymeric fibers with nanostructured silver coatings by ionized jet deposition for antibacterial tissues, Mater. Sci. Eng. C Mater. Biol. Appl. 113 (2020) 110998.
[50] D. Ghezzi, M. Boi, E. Sassoni, F. Valle, E. Giusto, E. Boanini, N. Baldini, M. Cappelletti, G. Graziani, Customized biofilm device for antibiofilm and antibacterial screening of newly developed nanostructured silver and zinc coatings, J. Biol. Eng. 17 (1) (2023) 18.
[51] D. Ghezzi, E. Sassoni, M. Boi, M. Montesissa, N. Baldini, G. Graziani, M. Cappelletti, Antibacterial and antibiofilm activity of nanostructured copper films prepared by ionized jet deposition, Antibiotics 12 (1) (2023) 55.
[52] G. Graziani, K. Barbaro, I.V. Fadeeva, D. Ghezzi, M. Fosca, E. Sassoni, G. Vadalà, M. Cappelletti, F. Valle, N. Baldini, J.V. Rau, Ionized jet deposition of antimicrobial and stem cell friendly silver-substituted tricalcium phosphate nanocoatings on titanium alloy, Bioact. Mater. 6 (8) (2021) 2629–2642.
[53] V. La Torre, E. Rambaldi, G. Masi, S. Nici, D. Ghezzi, M. Cappelletti, M.C. Bignozzi, Validation of antibacterial systems for sustainable ceramic tiles, Coatings 11 (11) (2021) 1409.
[54] Y.N. Slavin, J. Asnis, U.O. Häfeli, H. Bach, Metal nanoparticles: understanding the mechanisms behind antibacterial activity, J. Nanobiotechnol. 15 (1) (2017) 65.
[55] M. Akter, M.T. Sikder, M.M. Rahman, A. Ullah, K.F.B. Hossain, S. Banik, T. Hosokawa, T. Saito, M. Kurasaki, A systematic review on silver nanoparticles-induced cytotoxicity: physicochemical properties and perspectives, J. Adv. Res. 9 (2017) 1–16.
[56] M. Shevtsov, D. Gavrilov, N. Yudintceva, E. Zemtsova, A. Arbenin, V. Smirnov, I. Voronkina, P. Adamova, M. Blinova, N. Mikhailova, O. Galibin, M. Akkaoui, M. Pitkin, Protecting the skin-implant interface with transcutaneous silver-coated skin-and-bone-integrated pylon in pig and rabbit dorsum models, J. Biomed. Mater. Res. B Appl. Biomater. 109 (4) (2021) 584–595.
[57] Z. Ferdous, A. Nemmar, Health impact of silver nanoparticles: a review of the biodistribution and toxicity following various routes of exposure, Int. J. Mol. Sci. 21 (7) (2020) 2375.
[58] D. McShan, P.C. Ray, H. Yu, Molecular toxicity mechanism of nanosilver, J. Food Drug Anal. 22 (1) (2014) 116–127.
[59] M.C. Wyatt, M. Foxall-Smith, A. Roberton, A. Beswick, D.C. Kieser, M. R. Whitehouse, The use of silver coating in hip megaprostheses: a systematic review, Hip Int. 29 (1) (2019) 7–20.
[60] V.K. Sharma, C.M. Sayes, B. Guo, S. Pillai, J.G. Parsons, C. Wang, B. Yan, X. Ma, Interactions between silver nanoparticles and other metal nanoparticles under environmentally relevant conditions: a review, Sci. Total Environ. 653 (2019) 1042–1051.
[61] https://health.ec.europa.eu/publications/nanosilver-safety-health-and-environmental-effects-and-role-antimicrobial-resistance_en.
[62] S. Marin, G.M. Vlasceanu, R.E. Triplea, I.R. Balor, M. Lemnaru, M.M. Marin, A.M. Grumezescu, Applications and toxicity of silver nanoparticles: a recent review.
[63] K. Sawicki, M. Czajka, M. Matysiak-Kucharek, B. Fal, B. Drop, S. Męczyńska-Wielgosz, K. Sikorska, M. Kruszewski, L. Kapka-Skrzypczak, Toxicity of metallic nanoparticles in the central nervous system, Nanotechnol. Rev. 8 (1) (2019) 175–200.
[64] EFSA Panel on Food Contact Materials, Enzymes and Processing Aids (CEP), C. Lambré, J.M. Barat Baviera, C. Bolognesi, A. Chesson, P.S. Cocconcelli, R. Crebelli, D.M. Gott, K. Grob, E. Lampi, M. Mengelers, A. Mortensen, I. L. Steffensen, C. Tlustos, H. Van Loveren, L. Vernis, H. Zorn, L. Castle, E. Di Consiglio, R. Franz, N. Hellwig, S. Merkel, M.R. Milana, E. Barthélémy, G. Rivière, Safety assessment of the substance silver nanoparticles for use in food contact materials, EFSA J. 19 (8) (2021) e06790.
[65] https://www.who.int/publications/i/item/9789241547604.
[66] https://www.efsa.europa.eu/en/efsajournal/pub/65a.
[67] M. van der Zande, R.J. Vandebriel, E. Van Doren, E. Kramer, Z. Herrera Rivera, C. S. Serrano-Rojero, E.R. Gremmer, J. Mast, R.J. Peters, P.C. Hollman, P. J. Hendriksen, H.J. Marvin, A.A. Peijnenburg, H. Bouwmeester, Distribution, elimination, and toxicity of silver nanoparticles and silver ions in rats after 28-day oral exposure, ACS Nano 6 (8) (2012) 7427–7442.
[68] P. Hartemann, P. Hoet, A. Proykova, T. Fernandes, A. Baun, W. De Jong, J. Filser, A. Hensten, C. Kneuer, J.Y. Maillard, H. Norppa, M. Scheringer, S. Wijnhoven, Nanosilver: safety, health and environmental effects and role in antimicrobial resistance, Mater. Today 18 (3) (2015) 122–123.
[69] M. Wu, L. Chen, R. Li, M. Dan, H. Liu, X. Wang, X. Wu, Y. Liu, L. Xu, L. Xie, Biodistribution and bio-availability of silver and gold in rat tissues with silver/gold nanorod administration, RSC Adv. 8 (22) (2018) 12260–12268.
[70] M. Tsukamoto, H. Miyamoto, Y. Ando, I. Noda, S. Eto, T. Akiyama, Y. Yonekura, M. Sonohata, M. Mawatari, Acute and subacute toxicity in vivo of thermal-sprayed silver containing hydroxyapatite coating in rat tibia, Biomed. Res. Int. 2014 (2014) 902343.
[71] A. Hashimoto, H. Miyamoto, T. Kobatake, T. Nakashima, T. Shobuike, M. Ueno, T. Murakami, I. Noda, M. Sonohata, M. Mawatari, The combination of silver-containing hydroxyapatite coating and vancomycin has a synergistic antibacterial effect on methicillin-resistant Staphylococcus aureus biofilm formation, Bone Joint Res. 9 (5) (2020) 211–218.
[72] T. Morimoto, H. Hirata, S. Eto, A. Hashimoto, S. Kii, T. Kobayashi, M. Tsukamoto, T. Yoshihara, Y. Toda, M. Mawatari, Development of silver-containing hydroxyapatite-coated antimicrobial implants for Orthopaedic and spinal surgery, Medicina (Kaunas) 58 (4) (2022) 519.
[73] M.M. Ghobashy, M.A. Elkodous, S.H. Shabaka, S.A. Younis, D.M. Alshangiti, M. Madani, S.A. Al-Gahtany, W.F. Elkhatib, A.M. Noreddin, N. Nady, G.S. El-Sayyad, An overview of methods for production and detection of silver nanoparticles, with emphasis on their fate and toxicological effects on human, soil, and aquatic environment, Nanotechnol. Rev. 10 (1) (2021) 954–977.
[74] J. Gallo, A. Panacek, R. Prucek, E. Kriegova, S. Hradilova, M. Hobza, M. Holinka, Silver nanocoating technology in the prevention of prosthetic joint infection, Materials (Basel) 9 (5) (2016) 337.